Journal of Mineralogical and Petrological Sciences, Volume 114, page 290–295, 2019

LETTER

Boron isotope compositions of antigorite-grade serpentinites in the Itoigawa-Omi area of the Hida-Gaien Belt, Japan

Chinatsu YAMADA*, Tatsuki TSUJIMORI**, Qing CHANG*** and Jun-Ichi KIMURA***

*Department of Earth Science, Graduate School of Science, Tohoku University, Sendai 980-8578, Japan
**Center for Northeast Asian Studies, Tohoku University, Sendai 980-8576, Japan
***Japan Agency for Marine-Earth Science and Technology (JAMSTEC), Yokosuka 237-0061, Japan

The antigorite-grade serpentinite and Late Paleozoic high-pressure schists are main components of a serpentinite-matrix mélange in the Itoigawa-Omi area, Hida-Gaien Belt, Japan. Based on the petrologic characteristics of the high-pressure schists, the mélange is divided into two units, namely an 'eclogitic unit' and a 'non-eclogitic unit'. Our preliminary in-situ boron isotope analyses of five serpentinites using a laser-ablation multiple-collector inductively-coupled-plasma mass spectrometry (LA-MC-ICPMS) found a systematic difference of boron isotopic trends among the two units in the same mélange. The 'eclogitic unit' serpentinites from Yunotani and Kotagi-gawa are characterized by lower δ^{11}B value (mostly lower than +10‰), whereas the non-eclogitic unit serpentinite from Omi-gawa is higher than +10‰. Although the δ^{11}B value of <0‰ was not measured from the eclogitic unit serpentinites, the relatively low δ^{11}B values of <+10‰ might have recorded the signature of fluids released from deep subducted dehydrating slab. In contrast, the non-eclogitic unit serpentinite might have been affected by fluids released from shallower portion. Our new data confirmed the potential sensitivity of the boron isotope signature of serpentinites reflecting variation of high-pressure metamorphism.

Keywords: Antigorite serpentinite, Boron isotope, Hida-Gaien Belt, Itoigawa-Omi area

INTRODUCTION

Boron is a fluid-mobile element with two stable isotopes (^{10}B and ^{11}B). Boron isotope fractionation is strongly affected by temperature, pH, and phase partitioning (e.g., Wunder et al., 2005; Konrad-Schmolke and Halama, 2014). In general, ^{11}B is preferentially partitioned into fluids with trigonal coordination, whereas ^{10}B is mainly partitioned into solids with tetrahedral coordination (Oi et al., 1989; Palmer and Swihart, 1996; Peacock and Hervig, 1999). Therefore, it has been known that boron is useful to quantify fluid transfer between the slab and the overlying mantle wedge in subduction zones. Serpentine minerals contain relatively high B concentration (e.g., Vils et al., 2011; Prigent et al., 2018). During last two decades, whole-rock and in-situ boron isotope analyses have been carried out on serpentinites in convergent margins around the world (e.g., Peacock and Hervig, 1999; Benton et al., 2001; Boschi et al., 2008; Vils et al., 2009; Scambelluri and Tonarini, 2012; Angiboust et al., 2014; Martin et al., 2016; Yamada et al., 2019). Particularly, Martin et al. (2016) characterized the two distinct origins of serpentinite in central Guatemala. In their study, serpentinites from the high-pressure mélange show low δ^{11}B values ranging from −14.4 to +9.7‰ in the same range as metamorphic blocks (−15.3 to +4.3‰), whereas serpentinites from the low-pressure ophiolite display high δ^{11}B values (0 to +18‰). They proposed an idea that the tectonic origin of serpentinites in a subduction zone can be discriminated based on boron isotopic composition. More recently, Yamada et al. (2019) also discriminated the Franciscan serpentinites, northern California into two groups using boron isotope composition. Serpentinites associated with blueschist-facies metamorphic rocks showed lower δ^{11}B value (−12 to +8.8‰) than blueschist-absent serpentinites (+7.2 to +24.4‰). The results indicate that blueschist-bearing serpentinites were affected by forearc slab fluids with lighter boron isotope signature in deeper conditions (>∼ 2 GPa). It also supports the effectiveness of boron isotope to identify the tectonic origin of serpentinites.

In order to evaluate the versatility of boron isotope reconnaissance for serpentinites associated with high-pressure metamorphic rocks, we investigated five serpentinites with two contrasting types of high-pressure metamorphic rocks in the Itoigawa-Omi area. We applied same method developed by Kimura et al. (2016) and used in Yamada et

doi:10.2465/jmps.190726
C. Yamada, chinatsu.yamada.r7@dc.tohoku.ac.jp Corresponding author
T. Tsujimori, tatsukix@tohoku.ac.jp

al. (2019). Here we report for the first time, the boron isotope compositions of serpentinites in the Hida-Gaien Belt.

GEOLOGIC SETTING

The Hida-Gaien Belt is a composite geotectonic unit that tectonically lies between the Hida Belt and the Mino-Tamba Belt (Fig. 1a). It consists of fragments of various pre-Jurassic geotectonic units widely developed in the Inner Zone of southwest Japan. Late Paleozoic high-pressure schists associated with jadeitite-bearing antigorite serpentinite and meta-serpentinite (Banno, 1958; Tsujimori et al., 2000; Kunugiza et al., 2004; Tsujimori, 2017; Tsujimori and Harlow, 2017) and Paleozoic to lower Mesozoic (Middle Ordovician to Upper Triassic) clastic rocks are the most characteristic components. The high-pressure schists of the Hida-Gaien Belt have been named the 'Renge Schists'; they mainly record greenschist- to amphibolite-facies metamorphism and locally preserve blueschist- to eclogite-facies metamorphism, indicating subduction zone metamorphism (Nakamizu et al., 1989; Tsujimori et al., 2000). In the Omi area, the Renge Schists are divided into two distinct groups: an 'eclogitic unit' and a 'non-eclogitic unit' (Tsujimori, 2002; Tsujimori and Matsumoto, 2006; Shinji and Tsujimori, 2019) (Fig. 1b). In the eclogitic unit (EC unit), glaucophane-bearing eclogite and garnet blueschist occur as mafic layers within paragonite-bearing metasedimentary schists; low-grade mafic schist commonly contains glaucophane and/or barroisite. The peak eclogite-facies condition was estimated as ~ 2.0-2.2 GPa and 550-600 °C (Tsujimori, 2002). Whereas, in the non-eclogitic unit (non-EC unit), garnet-amphibolites occur as layers and lens within garnet- and biotite-bearing metasedimentary schists (Matsumoto et al., 2011); the low-grade mafic schist contains actinolitic to hornblenditic amphiboles. Although blueschist- and eclogite-facies mineral assemblages have not yet been confirmed from the non-EC unit, prograde-zoned garnet porphyroblasts of garnet amphibolite include rare paragonite (Tsujimori and Matsumoto, 2006). The mineral assemblage suggests that the peak pressure condition of the non-EC unit garnet amphibolite was ~ 1 GPa lower than that of the EC unit at 550-600 °C (Tsujimori, 2002). Antigorite serpentinite occurs in both units. However, discrimination of serpentinites in the two units is difficult in terms of mineralogical and textural observation. A few differences include that some EC unit serpentinites are schistose and some non-EC unit serpentinites preserv relict chromian spinel (Tsujimori, 2004).

In this study, we investigated three serpentinites from Yunotani and Kotaki-gawa in the EC unit and two from Omi-gawa in the non-EC unit in the Itoigawa-Omi area (Fig. 1b).

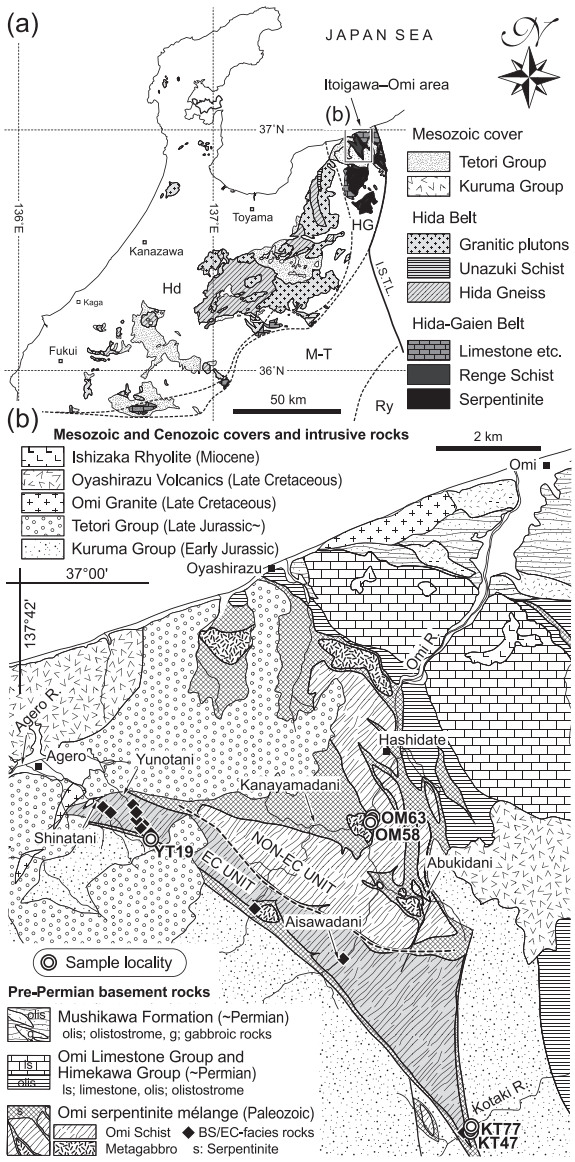

Figure 1. (a) Simplified geological map of the Hokuriku Region, showing location of the Itoigawa-Omi area (modified after Tsujimori, 2002). (b) A geological map of the Itoigawa-Omi area, showing sample localities (modified after Kumazaki and Kojima, 1996; Tsujimori, 2002). HG, Hida-Gaien Belt; Hd, Hida Belt; M-T, Mino-Tamba Belt; Ry, Ryoke Belt.

METHODS

Boron isotope ratios ($^{11}B/^{10}B$) were determined by a LA-MC-ICPMS at the Japan Agency for Marine-Earth Science and Technology (JAMSTEC). The OK Laboratory OK-EX2000 (OK Lab, Tokyo, Japan) 193-nm excimer laser ablation (193ExLA) system with a ~ 20 ns pulse duration at repetition rate of 5 Hz was used for the analyses. The 193ExLA was coupled to a modified Neptune (ThermoFisher Scientific, Bremen, Germany) MC-ICPMS. The spot diameter was 200 μm and ~ 35 μm depth

crater was generated after single spot analysis. Mass bias correction was carried out by standard-sample bracketing method using the SRM 612 synthetic glass ($^{11}B/^{10}B$ = 4.042; Jochum and Stoll, 2008) provided by the National Institute of Standard and Technology (NIST). We used the same method as presented in Kimura et al. (2016), which enabled accurate boron isotope ratio analyses of various materials with different matrix; see the details of analytical protocol in Kimura et al. (2016) and an example of application using the same method as Yamada et al. (2019). Isotopic compositions for B are normalized to the reference isotope composition $^{11}B/^{10}B = 4.048$ (Catanzaro et al., 1970) of NIST® SRM 951 boron acid by $\delta^{11}B = [(^{11}B/^{10}B)_{sample}/(^{11}B/^{10}B)_{SRM951}-1] \times 1000$. Both the reproducibility and the laboratory bias of $\delta^{11}B$ measurements were within ±1‰ (2SD). We also measured the solid rock slabs of JB-2 basalt to check the data quality. The JB-2 yielded an average $\delta^{11}B$ of +7.04‰, consistent with literature values (e.g., +7.24 ± 0.33‰: Brand et al., 2014).

Identification of serpentine minerals was performed by HORIBA XploRA PLUS Confocal Raman Microscope at the Graduate School of Environmental Studies, Tohoku University. A 532 nm solid-state Nd-YAG laser with 10 mW power was used as the light source. The Raman Spectra were measured ranging from 200 to 1194 cm^{-1} and 3446 to 3922 cm^{-1} in 1.1 cm^{-1} steps (2400 gr/mm). The measured area is ~ 2 μm; the exposure time is 50s (5s × 10). The Raman shift was calibrated using a reference silicon.

PETROGRAPHIC FEATURES OF SAMPLES

The textures of each serpentinite are shown in Figure 2. The Yunotani sample (YT19) is a weakly schistose serpentinite, consisting of mainly antigorite with a small amount of chlorite and magnetite. Raman spectrum of antigorite shows diagnostic peaks at 232, 375, 527, 1040, and 3665 cm^{-1} with a weak inflection at 3619 cm^{-1} and ~ 3698 cm^{-1} (Petriglieri et al., 2015) (Fig. 3a). The Kotaki-gawa samples (KT47 and KT77) were collected from outcrops near barroisite-bearing mafic schist. It consists mainly of antigorite with chlorite, brucite and minor amount of dolomite, pentlandite, and magnetite. Antigorite is partially replaced by lizardite. The Omi-gawa samples (OM58 and OM63) are massive antigorite serpentinites with pseudomorphic texture after olivine. Although the samples do not preserve relict olivine, the abundant mesh-texture without bastite texture suggests a dunite-origin. The samples contain a minor amount of magnetite and chlorite after chromite, and antigorite is replaced by lizardite. Tsujimori (2004) reported relict high-Cr chromite in a serpentinite boulder derived from the same outcrop of OM58 and OM63. The relict chromite is remarkably zoned from the chromite core [Cr/(Cr + Al) = 0.75-0.77] to the ferritchromite rim and contains up to 0.3 wt% TiO_2 in the cores. The high-Ti and compositional zoning support that the serpentinite along the Omi-gawa was metamorphosed serpentinite of dunite-origin. Although Yokoyama (1985) found metamorphic olivine, our study could not confirm it. Raman spectrum of retrograde lizardite shows diagnostic peaks at 226, 380, 685, 3683, and 3701 cm^{-1} with a weak inflection at 346 cm^{-1} and ~ 3656 cm^{-1} (Petriglieri et al., 2015) (Fig. 3b).

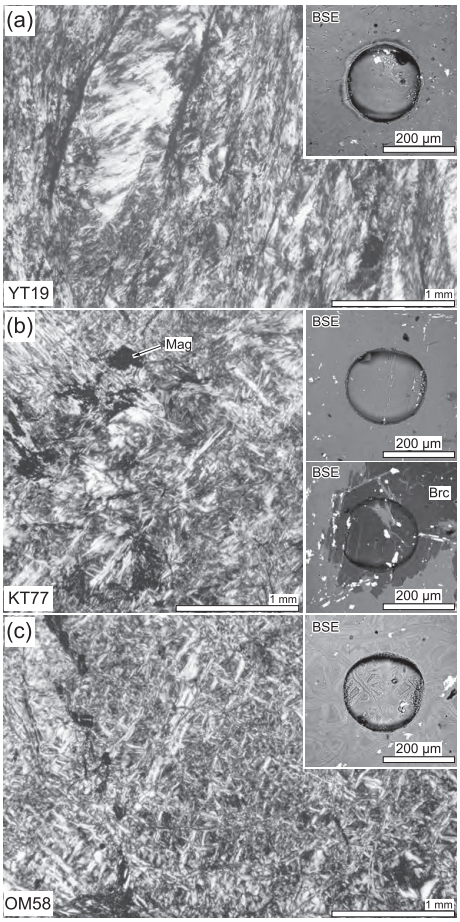

Figure 2. Representative microtextures (cross-polarized photomicrographs) of (a) Yunotani (YT19), (b) Kotaki-gawa (KT77), and (c) Omi-gawa (OM58) serpentinites. Scale bars represent 1 mm. All minerals without a label are serpentines. Back-scattered electron images of representative laser ablation craters are also shown in Figure 2. Mag, magnetite; Brc, brucite.

BORON ISOTOPES OF SERPENTINITES

Table 1 shows the 40 spot analyses for 5 samples from Yunotani (YT19), Kotaki-gawa (KT47 and KT77) and Omi-gawa (OM58 and OM63). Note that the Kotaki-gawa sample (KT77) includes one analysis of brucite. The back-scattered electron images of representative laser ablation

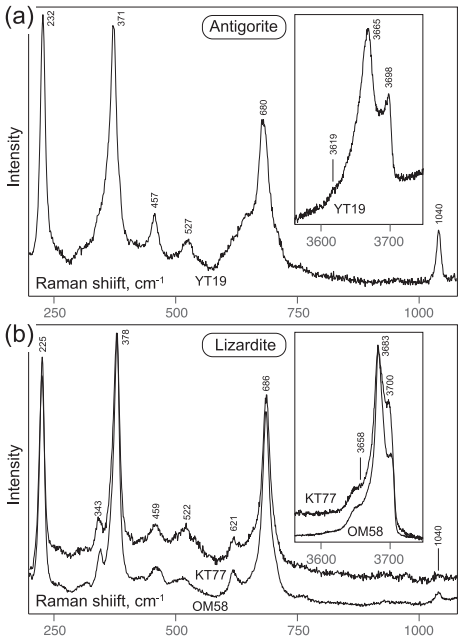

Figure 3. Raman spectrum of (a) antigorite in the Yunotani serpentinite (YT19) and (b) retrograde lizardites of the Kotaki-gawa (KT77) and Omi-gawa (OM58) serpentinites.

craters are also shown in Figure 2. Boron concentration and $\delta^{11}B$ value of the analyzed samples were vary widely, ranging from 9.1 to 315 $\mu g \cdot g^{-1}$ and +6.2 to +14.9‰, respectively (Fig. 4). The Yunotani sample (YT19) of the EC unit shows moderate boron concentration (12.5-48.4 $\mu g \cdot g^{-1}$) with relatively low $\delta^{11}B$ value (+6.6-+12.3‰, mostly <+9‰). Two EC unit serpentinites from Kotaki-gawa are characterized by very high boron [200-315 $\mu g \cdot g^{-1}$ (KT77)] and moderate boron concentration [18-123 $\mu g \cdot g^{-1}$ (KT47)]. The two serpentinites show similar range of $\delta^{11}B$ (+6.2-+12.7‰, mostly <+10‰). Brucite in KT77 is characterized by lower boron concentration (37.5 $\mu g \cdot g^{-1}$) but similar $\delta^{11}B$ value (+5.8‰) to those of serpentine. Notably, the boron isotope range of the Kotaki-gawa serpentinite overlaps with that of the Yunotani serpentinite.

In contrast, the non-EC unit serpentinites from the Omi-gawa (OM58 and OM63) yielded a wide range of boron concentration (9.1-147 $\mu g \cdot g^{-1}$) and relatively high $\delta^{11}B$ values (+11.6-+19.5‰, mostly >+14‰) than those of the EC unit serpentinite.

DISCUSSION

As shown in Figure 4, the systematic difference of boron isotopic trends is confirmed between the two units in the same mélange. The EC unit serpentinites from Yunotani and Kotagi-gawa are characterized by lower $\delta^{11}B$ value (or mostly smaller than +10‰) than the non-EC unit serpentinites (or mostly higher than +14‰).

Table 1. Boron isotope compositions for the studied serpentinites

Sample_#spot ID	B ($\mu g \cdot g^{-1}$)	2σ	$\delta^{11}B$ (‰)	2σ
Yunotani (eclogite unit)				
YT19_#01	19.4	2.3	+6.6	0.7
YT19_#02	17.6	1.9	+7.2	0.6
YT19_#03	25.7	4.2	+8.0	0.6
YT19_#04	17.8	1.3	+8.7	0.6
YT19_#05	20.2	1.5	+8.0	0.7
YT19_#06	17.7	1.3	+12.3	0.8
YT19_#07	40.0	17.4	+8.2	0.7
YT19_#08	12.5	0.4	+7.1	1.0
YT19_#09	22.0	0.8	+6.6	0.7
YT19_#10	48.4	5.2	+8.1	0.5
Kotaki-gawa (eclogite unit)				
KT47_#01	74.6	3.5	+8.3	0.4
KT47_#02	57.3	8.2	+10.1	0.4
KT47_#03	18.1	1.6	+9.0	0.5
KT47_#04	123.7	4.9	+12.7	0.4
KT47_#05	65.9	3.0	+9.8	0.4
KT77_#01	264.7	9.5	+9.2	0.5
KT77_#02	277.9	12.8	+10.7	0.5
KT77_#03	315.4	11.8	+8.3	0.4
KT77_#04	272.5	7.6	+6.9	0.4
KT77_#05	302.0	8.7	+6.5	0.4
KT77_#06	200.0	10.7	+8.0	0.5
KT77_#07	272.9	7.9	+7.9	0.5
KT77_#08	284.2	6.8	+7.3	0.6
KT77_#09	300.0	12.5	+6.3	0.7
KT77_#10(brucite)	37.5	1.9	+5.8	0.6
Omi-gawa (non-eclogite unit)				
OM58_#01	68.0	1.4	+13.6	0.5
OM58_#02	86.8	4.7	+14.9	0.5
OM58_#03	95.7	2.4	+14.9	0.4
OM58_#04	97.1	10.1	+14.3	0.4
OM58_#05	98.5	4.5	+13.6	0.5
OM58_#06	135.5	2.8	+14.2	0.7
OM58_#07	133.1	3.3	+14.2	0.7
OM58_#08	135.9	5.4	+14.1	0.7
OM58_#09	9.1	0.6	+11.6	1.3
OM58_#10	145.0	4.4	+13.4	0.6
OM63_#01	26.0	1.7	+14.7	0.6
OM63_#02	14.6	0.7	+15.5	0.6
OM63_#03	46.4	5.3	+15.1	3.5
OM63_#04	35.1	2.3	+15.6	0.5
OM63_#05	146.7	7.3	+19.5	0.5
JB-2_#1	33.5	1.1	+6.3	0.7
JB-2_#2	24.6	2.0	+6.8	0.6
JB-2_#3	73.7	10.2	+8.4	0.5
JB-2_#4	63.0	2.6	+6.9	0.5
JB-2_#5	64.4	3.1	+6.8	0.5

The $\delta^{11}B$ values of the EC unit serpentinites from Yunotani and Kotaki-gawa overlap with those of the Franciscan blueschist-bearing serpentinites, especially

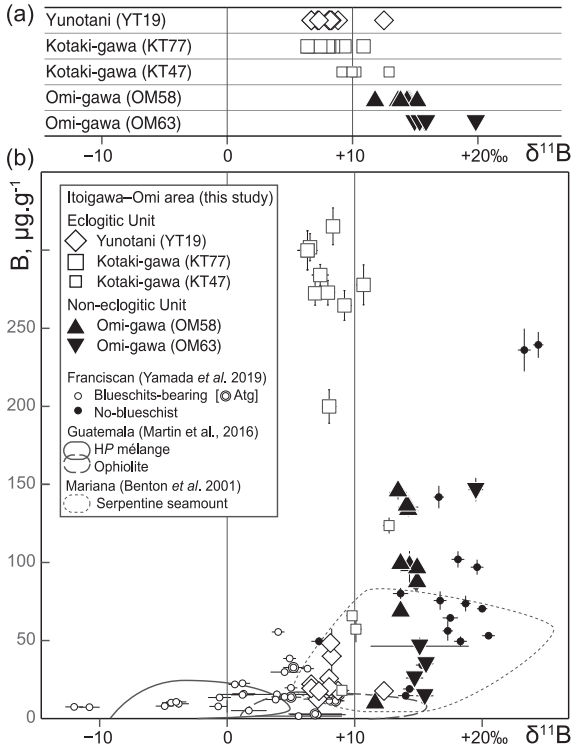

Figure 4. Summary of $\delta^{11}B$ of the studied serpentinites from the Itoigawa-Omi area. (a) Variations of $\delta^{11}B$ of each sample. Note that open symbols represent serpentinites of the 'eclogitic unit' and the filled triangle symbol represents serpentinite of the 'non-eclogitic unit'. (b) $\delta^{11}B$ versus boron concentration diagram showing compositional variations of the studied area. For comparisons, compositional trends from the Franciscan Complex of northern California (Yamada et al., 2019), the Motagua Suture Zone of Guatemala (Martin et al., 2016) and Mariana forearc (Benton et al., 2001) are also shown.

of antigorite serpentinites. However, we could not detect the $\delta^{11}B$ value of <0‰ from the EC unit serpentinites. It is also important that the very high $\delta^{11}B$ values up to +20‰ are also not found in the non-EC unit serpentinites. It has been known that the boron isotope fractionation is more significant at lower temperature condition (Wunder et al., 2005). In our study in the Franciscan Complex (Yamada et al., 2019), serpentinites with very low $\delta^{11}B$ value are associated with low-temperature lawsonite blueschist. In contrast, the EC unit serpentinites of the Itoigawa-Omi area bear much higher grade blueschist and rare eclogite. This fact might explain the regional difference of the lowest $\delta^{11}B$ values in those two regions.

Some experiments and geochemical modeling proposed the behavior of boron released from a subducting slab during progressive dehydration (e.g., Peacock and Hervig, 1999; Wunder et al., 2005; Marschall et al., 2007; Konrad-Schmolke and Halama, 2014). These studies conclude that boron concentration and $\delta^{11}B$ value will decrease with increasing depth because of the strong fractionation of ^{11}B into the fluid phase. Using the Arc Basalt Simulator version 3 (ABS3) code (Kimura et al., 2010), Yamada et al. (2019) calculated systematic changes of boron concentration and boron isotopic composition for different slab materials and slab fluids of an oceanic plate subduction. They expected the presence of slab fluids with high $\delta^{11}B$ value >~ +15‰ in the depth of <~ 2 GPa (see Fig. 7 of Yamada et al., 2019). However, the further dehydration of the subducting slab releases fluids with $\delta^{11}B$ lower than +10 ‰ in the depth of >~ 2.5 GPa. The observed $\delta^{11}B$ signature of the EC unit serpentinites might have affected by the upward fluids released from the subducting slab in the depth of >~ 2.5 GPa. In this sense, the non-EC unit serpentinites might have been formed at shallower portion where fluid with heavier ^{11}B is active. Another alternative idea is that primary low $\delta^{11}B$ signature gained from a deep slab fluid was overprinted by heavy boron at a shallow depth during retrogression. In any case, our preliminary data in this study found the systematic boron isotopic difference between the EC unit and the non-EC unit serpentinites. In short, this study confirmed the potential sensitivity of the boron isotope signature of serpentinites reflecting variation of high-pressure metamorphism.

ACKNOWLEDGMENTS

This research was supported by the Center for Northeast Asian Studies, Tohoku University and the Japan Agency for Marine-Earth Science and Technology (JAMSTEC) in part by MEXT/JSPS KAKENHI Grant Numbers JP15H05212 and JP18H01299 to T. Tsujimori and JP15H02148, JP16H01123, and JP18H04372 to J.-I. Kimura. We appreciate for constructive reviews from Tsuyoshi Ishikawa and Yuji Ichiyama. We extend our appreciation to Uno Masaoki and Noriyoshi Tsuchiya for their assistance on Raman spectroscopy. We thank Naoko Takahashi, Daniel Pastor-Galán and Kennet E. Flores for feedback.

REFERENCES

Angiboust, S., Pettke, T., De Hoog, J.C., Caron, B. and Oncken, O. (2014) Channelized fluid flow and eclogite-facies metasomatism along the subduction shear zone. Journal of petrology, 55, 883-916.

Banno, S. (1958) Glaucophane schists and associated rocks in the Omi district, Niigata Prefecture, Japan. Japanese Journal of Geology and Geography, 29, 29-44.

Benton, L.D., Ryan, J.G. and Tera, F. (2001) Boron isotope systematics of slab fluids as inferred from a serpentine seamount, Mariana forearc. Earth and Planetary Science Letters, 187, 273-282.

Boschi, C., Dini, A., Früh-Green, G.L. and Kelley, D.S. (2008) Isotopic and element exchange during serpentinization and

metasomatism at the Atlantis Massif (MAR 30 N): insights from B and Sr isotope data. Geochimica et Cosmochimica Acta, 72, 1801-1823.

Brand, W.A., Coplen, T.B., Vogl, J., Rosner, M. and Prohaska, T. (2014) Assessment of international reference materials for isotope-ratio analysis (IUPAC Technical Report). Pure and Applied Chemistry, 86, 425-467.

Catanzaro, E.J., Champion, C.E., Garner, E.L., Marinenko, G., et al. (1970) Standard Reference Materials: Boric acid; isotopic, and assay standard reference materials. In NBS Special Publication 260-17, pp. 70, National Bureau of Standards, Boulder.

Jochum, K.P. and Stoll, B. (2008) Reference materials for elemental and isotopic analyses by LA-(MC)-ICP-MS: Successes and outstanding needs. Laser Ablation ICP-MS in the Earth Sciences: Current practices and outstanding issues, 40, 147-168.

Kimura, J.I., Kent, A.J., Rowe, M.C., Katakuse, M., et al. (2010) Origin of cross-chain geochemical variation in Quaternary lavas from the northern Izu arc: Using a quantitative mass balance approach to identify mantle sources and mantle wedge processes. Geochemistry, Geophysics, Geosystems, 11, doi:10.1029/2010GC003050.

Kimura, J.I., Chang, Q., Ishikawa, T. and Tsujimori, T. (2016) Influence of laser parameters on isotope fractionation and optimisation of lithium and boron isotope ratio measurements using laser ablation-multiple Faraday collector-inductively coupled plasma mass spectrometry. Journal of Analytical Atomic Spectrometry, 31, 2305-2320.

Konrad-Schmolke, M. and Halama, R. (2014) Combined thermodynamic-geo-chemical modeling in metamorphic geology: Boron as tracer of fluid-rock interaction. Lithos, 220, 393-414.

Kumazaki, N. and Kojima, S. (1996) Depositional history and structural development of the Kuruma Group (lower Jurassic) on the basis of clastic rock composition. Journal of the Geological Society of Japan, 102, 285-302.

Kunugiza, K., Goto, A., Itaya, T. and Yokoyama, K. (2004) Geological development of the Hida Gaien belt: Constraints from K-Ar ages of high P/T metamorphic rocks and U-Th-Pb EMP ages of granitic rocks affecting contact metamorphism of serpentinite. Journal of the Geological Society of Japan, 110, 580-590.

Marschall, H.R., Altherr, R. and Rüpke, L. (2007) Squeezing out the slab—Modelling the release of Li, Be and B during progressive high-pressure metamorphism. Chemical Geology, 239, 323-335.

Matsumoto, K., Sugimura, K., Tokita, I., Kunugiza, K. and Maruyama, S. (2011) Geology and Metamorphism of the Itoigawa-Omi Area of the Hida Gaien Belt, Central Japan. Journal of Geography, 120, 4-29.

Martin, C., Flores, K.E. and Harlow, G.E. (2016) Boron isotopic discrimination for subduction-related serpentinites. Geology, 44, 899-902.

Nakamizu, M., Okada, M., Yamazaki, T. and Komatsu, M. (1989) Metamorphic rocks in the Omi-Renge serpentinite melange, Hida Marginal Tectonic Belt, Central Japan. Memoirs of the Geological Society of Japan, 33, 21-35.

Oi, T., Nomura, M., Musashi, M., Osaka, T., et al. (1989) Boron isotopic compositions of some boron minerals. Geochimica et Cosmochimica Acta, 53, 3189-3195.

Palmer, M.R. and Swihart, G.H. (1996) Boron isotope geochemistry: an overview. Reviews in Mineralogy and Geochemistry, 33, 709-744.

Peacock, S.M. and Hervig, R.L. (1999) Boron isotopic composition of subduction-zone metamorphic rocks. Chemical Geology, 160, 281-290.

Petriglieri, P.J., Salvioli-Mariani, E., Mantovani, L., Tribaudino, M., et al. (2015) Micro-Raman mapping of the polymorphs of serpentine. Journal of Raman Spectroscopy, 46, 953-958.

Prigent, C., Guillot, S., Lemarchand, D., Soret, M. and Ulrich, M. (2018) Transfer of subduction fluids into the deforming mantle wedge during nascent subduction: Evidence from trace elements and boron isotopes (Semail ophiolite, Oman). Earth and Planetary Science Letter, 484, 213-228.

Scambelluri, M. and Tonarini, S. (2012) Boron isotope evidence for shallow fluid transfer across subduction zones by serpentinized mantle. Geology, 40, 907-910.

Shinji, Y. and Tsujimori, T. (2019) Retrograde pumpellyite in the Yunotani garnet blueschist of the Omi area, Japan: An update on the cooling path. Journal of Mineralogical and Petrological Sciences, 114, 26-32.

Tsujimori, T. (2002) Prograde and retrograde PT paths of the late Paleozoic glaucophane eclogite from the Renge metamorphic belt, Hida Mountains, southwestern Japan. International Geology Review, 44, 797-818.

Tsujimori, T. (2004) Origin of serpentinites in the Omi serpentinite melange (Hida Mountains, Japan) deduced from zoned Cr-spinel. Journal of the Geological Society of Japan, 110, 591-597.

Tsujimori, T. (2017) Early Paleozoic jadeitites in Japan: An overview. Journal of Mineralogical and Petrological Sciences, 112, 217-226.

Tsujimori, T., Ishiwatari, A. and Banno, S. (2000) Eclogitic glaucophane schist from the Yunotani valley in Omi Town, the Renge metamorphic belt, the Inner Zone of southwestern Japan. Journal of the Geological Society of Japan, 106, 353-362.

Tsujimori, T. and Matsumoto, T. (2006) P-T pseudosection of a glaucophane-epidote eclogite from Omi serpentinite mélange, SW Japan: a preliminary report. Journal of the Geological Society of Japan, 112, 407-414.

Tsujimori, T. and Harlow, G.E. (2017) Jadeitite (jadeite jade) from Japan: History, characteristics, and perspectives. Journal of Mineralogical and Petrological Sciences, 112, 184-196.

Vils, F., Tonarini, S., Kalt, A. and Seitz, H.M. (2009) Boron, lithium and strontium isotopes as tracers of seawater-serpentinite interaction at Mid-Atlantic ridge, ODP Leg 209. Earth and Planetary Science Letters, 286, 414-425.

Vils, F., Müntener, O., Kalt, A. and Ludwig, T. (2011) Implications of the serpentine phase transition on the behavior of beryllium and lithium-boron of subducted ultramafic rocks. Geochimica et Cosmochimica Acta, 75, 1249-1271.

Wunder, B., Meixner, A., Romer, R.L., Wirth, R. and Heinrich, W. (2005) The geochemical cycle of boron: constraints from boron isotope partitioning experiments between mica and fluid. Lithos, 84, 206-216.

Yamada, C., Tsujimori, T., Chang, Q. and Kimura, J.I. (2019) Boron isotope variations of Franciscan serpentinites, northern California. Lithos, 334, 180-189.

Yokoyama, K. (1985) Ultramafic rocks in the Hida marginal zone. Memoirs of the National Science Museum Tokyo, 18, 5-18.

Manuscript received July 26, 2019
Manuscript accepted November 6, 2019

Manuscript handled by M. Satish-Kumar